

Cosmic superstring trajectories in warped compactifications

Anastasios Avgoustidis^{1*}, Sarah Chadburn^{2†}, and Ruth Gregory^{2,3‡}

¹*School of Physics and Astronomy, University of Nottingham,
University Park, Nottingham NG7 2RD, UK*

²*Centre for Particle Theory, Durham University,
South Road, Durham, DH1 3LE, UK*

⁴*Perimeter Institute, 31 Caroline St, Waterloo, Ontario N2L 2Y5, Canada*

ABSTRACT: We explore the generic motion of cosmic (super)strings when the internal compact dimensions are warped, using the Klebanov-Strassler solution as a prototypical throat geometry. We find that there is no dynamical mechanism which localises the string at the tip of the throat, but rather that the motion seems to explore both internal and external degrees of freedom democratically. This indicates that cosmic (super)strings formed by inflationary brane-antibrane annihilation will have sufficient internal motion for the gravitational wave signals from the string network to be suppressed relative to the signal from a ‘standard’ cosmic string network.

KEYWORDS: Extra Dimensions, Cosmic Superstrings.

*Email: a.avgoustidis@damtp.cam.ac.uk

†Email: s.e.chadburn@durham.ac.uk

‡Email: r.a.w.gregory@durham.ac.uk

Contents

1. Introduction	1
2. Strings on a warped internal manifold	3
3. String motion in a static spacetime	6
3.1 A simple Ansatz	8
3.2 More general loops	11
3.3 Effect of two-form charges	15
4. Cosmological loops	16
4.1 Cosmological expansion	17
4.2 Gravitational radiation	21
5. Discussion	23

1. Introduction

Cosmic strings, [1], have had a checkered past in terms of their relevance or popularity in particle cosmology. Initially, these strings were relic topological defects of some Grand Unified phase transition in the early universe, [2], and proposed as an alternative to inflation. However, the microwave background perturbations show that strings cannot be responsible for structure formation, [3], although can nonetheless be present as a sub-dominant component, [4]. Recently, cosmic strings have had a renaissance as by-products of string theoretic brane inflationary scenarios [5, 6, 7, 8, 9]. The basic picture here is that inflation is driven by a mobile D-brane in a warped extra dimension scenario. Inflation ends (typically) by brane/anti-brane annihilation, a by-product of which are cosmic superstrings, [9]. Although, when formed, these objects are inherently string theoretic, and can have interesting and distinctive properties, it is assumed that they persist to low energies as topological defects somewhat similar to the more traditional cosmic strings. As such, if detected, they could provide indirect evidence of string theory [10, 11].

The basic cosmological picture is that cosmic strings form a network of loops and long strings, whose evolution is determined by rules for intercommutation [12],

or how crossing strings interact, and an effective action governing the motion of the string, which is well approximated by the zero width action, [13, 14]:

$$S = -\mu \int d^2\sigma \sqrt{\gamma} \quad (1.1)$$

where μ is the mass per unit length of the string, and γ_{AB} the induced metric on the worldsheet. Incorporating gravitational effects via a linearized approximation indicates how fast energy is lost from the network, [15, 16], and putting all these pieces together gives a scaling behaviour for the string network, [17]. Cosmic (super)strings, [18], are generally modelled in a similar fashion, but have some interesting differences as they are derived from a higher dimensional theory, string theory, and have additional physics arising as a result. The most important difference is that these strings need not intercommute when they apparently intersect in our 4D world, [19], resulting in a denser network, [9, 20, 21]. Cosmic superstrings can also have junctions, [19, 22, 23, 24], although the implications for the network have been less well explored. For recent progress, both on the numerical and analytic fronts, see [25, 26, 27].

The particular phenomenon we are interested in in this paper is the effect of the extra dimensions on the kinematics of the string network. The motion of the string can be thought of as left and right moving waves along the string, [28], thus if there is internal motion, the projection of these waves onto our non-compact four-dimensional spacetime leads to a lower apparent velocity, [29]. (This effect is analogous to string currents in superconducting strings [30, 31, 32].) While this does not have so strong an effect on the shape of general loops, the impact on highly relativistic events such as cusps is dramatic. Cusps are transitory events, where constructive interference between the left and right moving modes causes a point of the string instantaneously to reach the speed of light, however, if the strings are moving slower, they will not only fail to reach the speed of light instantaneously in the noncompact dimensions, but in fact also have a reduced probability of such a relativistic event occurring. Another singular feature of cosmic string motion are kinks, or sharp ‘corners’ on the string representing a discontinuity in the wave velocity. They are formed as relics of intercommutation, and because they are a feature of only one wavefront, they persist and move along the string, [33].

Since both kinks and cusps represent a certain level of singularity of the worldsheet swept out by the string, when including gravitational backreaction they generate strong and distinct gravitational wave signals, [15, 16, 34, 35, 36, 37], which have been used to place bounds on the tension of the string and the inflationary scenario, [38]. Recently, [39, 40], the implication of the motion in the extra dimensions was explored by modelling the extra dimensions as flat, and considering the impact of the reduced wave velocity in the non-compact directions. The cusp signal was found to be significantly damped, primarily due to the fact that motion in higher dimensions

has a significantly reduced probability of cusp formation. The kink signal was also reduced, though less dramatically. In each case, a reduction in signal can be linked to the presence of internal velocities, thus any possible mechanism which would damp or dry out motion in the internal dimensions would significantly alter our previous conclusions.

In this paper, we consider the impact of warped internal dimensions on the motion of the cosmic superstrings. It is commonly asserted that the warping of spacetime causes cosmic strings to be localised in the internal dimensions; that is, at late times, their positions can be expected to get fixed at the tip of the warped throat, with no freedom to move on the internal manifold. This can be understood by noting that the string positions in the internal dimensions are worldsheet scalar fields [30], which have a massive potential in the presence of warping. At low energies therefore, one might expect that such additional fields would acquire masses and stabilise, presumably corresponding to the string lying at the bottom of the warped throat. However, it is not entirely clear that the string can be dynamically stabilised at the potential bottom in the absence of a strong damping mechanism for internal excitations [41]. Moreover, if the string is displaying characteristics derived from its higher dimensional inheritance, such as a low intercommutation probability, then it seems entirely possible that it will also display other consequences of its higher dimensional nature, such as these internal degrees of freedom. In the absence of an explicit concrete construction of the low energy degrees of freedom, it seems reasonable to explore the consequence of internal motion for the cosmic string.

Here, we examine this issue in more detail by studying the classical motion of strings in warped spacetimes. This is motivated by the fact that, in many realistic compactifications, the relevant compactification scales can be much larger than the string scale, which sets the scale of the string thickness. Thus, at late times, when the strings are part of a cosmological network and are effectively topological defects existing at low energies, it seems reasonable to assume that if they are semi-classical objects as far as our 4D universe is concerned, then they also have a semi-classical nature in the extra dimensions. We therefore allow for the string to be free to move in the internal dimensions, and study the dynamics of string loops in a warped throat modelled by the Klebanov-Strassler (KS) solution [42]. We find that, although there is an attractive force towards the bottom of the throat, there is no friction to ensure stabilisation. On the contrary, there is continuous exchange of energy between the external and internal sectors, reinforcing motion in the internal manifold. This provides strong evidence that string loops can have significant motion in the internal dimensions, even in a strongly warped spacetime.

2. Strings on a warped internal manifold

In order to explore the effect of warped internal dimensions on the motion of the

string, we use the concrete example of the warped deformed conifold, or Klebanov-Strassler, solution [42]. This is an exact supergravity solution with D3 and wrapped D5 branes, which interpolates from a regular $\mathbb{R}^3 \times S^3$ tip, to an $\mathbb{R} \times T^{1,1}$ cone in the UV. The ten dimensional metric is:

$$ds_{10}^2 \equiv G_{ab} dx^a dx^b = h^{-1/2} g_{\mu\nu} dx^\mu dx^\nu - h^{1/2} \tilde{g}_{mn} dy^m dy^n, \quad (2.1)$$

where $g_{\mu\nu}(x)$ is the 4D spacetime metric and $\tilde{g}_{mn}(y)$ the 6D internal metric, whose explicit form will be given below. The warp factor, h , depends only on the radial internal direction η (see Eq. (2.4) below), and is given by:

$$h = 2(g_s M \alpha')^2 \epsilon^{-8/3} I(\eta), \quad (2.2)$$

where

$$I(\eta) \equiv \int_\eta^\infty dx \frac{x \coth x - 1}{\sinh^2 x} (\sinh x \cosh x - x)^{1/3}. \quad (2.3)$$

Here M is a compactification parameter representing the number of dissolved D5 branes in the background, and ϵ is a dimensionful parameter measuring the deformation of the conifold. The string coupling and string scale are given as usual by g_s and α' .

Our four-dimensional spacetime $g_{\mu\nu} dx^\mu dx^\nu$ will be taken either to be Minkowski spacetime, as in the original KS solution, or an FRW universe, when we consider the effect of cosmological expansion. The internal manifold is the warped throat, and has the form:

$$\tilde{g}_{mn} dy^m dy^n = \frac{\epsilon^{4/3}}{2} K(\eta) \left[\frac{1}{3K(\eta)^3} \{d\eta^2 + (g^5)^2\} + \cosh^2 \frac{\eta}{2} \{(g^3)^2 + (g^4)^2\} + \sinh^2 \frac{\eta}{2} \{(g^1)^2 + (g^2)^2\} \right], \quad (2.4)$$

where η is a radial coordinate in which the other metric functions have analytic expressions

$$K(\eta) = \frac{(\sinh \eta \cosh \eta - \eta)^{1/3}}{\sinh \eta}. \quad (2.5)$$

The g^i 's are forms representing the angular directions, typically expressed by

$$g^{1,3} = \frac{e^1 \mp e^3}{\sqrt{2}}, \quad g^{2,4} = \frac{e^2 \mp e^4}{\sqrt{2}}, \quad g^5 = e^5 \quad (2.6)$$

with

$$\begin{aligned} e^1 &= -\sin \theta_1 d\phi_1, & e^2 &= d\theta_1, & e^3 &= \cos \psi \sin \theta_2 d\phi_2 - \sin \psi d\theta_2, \\ e^4 &= \sin \psi \sin \theta_2 d\phi_2 + \cos \psi d\theta_2, & e^5 &= d\psi + \cos \theta_1 d\phi_1 + \cos \theta_2 d\phi_2. \end{aligned} \quad (2.7)$$

(For details on the warped deformed conifold, and coordinate systems, see e.g. [42, 43].)

In addition, there are NSNS and RR fluxes in the throat, given by

$$B_2 = g_s M \frac{(\eta \coth \eta - 1)}{2 \sinh \eta} [(\cosh \eta - 1)g^1 \wedge g^2 + (\cosh \eta + 1)g^3 \wedge g^4] \quad (2.8)$$

$$F_3 = \frac{M}{2} [2g^3 \wedge g^4 \wedge g^5 + d((1 - \eta \operatorname{csch} \eta)[g^1 \wedge g^3 + g^2 \wedge g^4])] . \quad (2.9)$$

The exact KS solution is an infinite throat, however, it is presumed to be a good approximation to a finite throat glued to a compact Calabi-Yau internal manifold at some UV scale $r_{UV} \simeq \epsilon^{2/3} \int_0^{\eta_{UV}} d\eta / \sqrt{6} K$. This scale sets the UV/IR hierarchy of the throat $h_0/h_{UV} \sim 0.302 e^{\frac{4}{3}\eta_{UV}} / \eta_{UV}$, and the size of the internal manifold. This latter relation provides a lower bound on the four dimensional Planck scale in terms of the string scale and compactification parameters

$$M_p^2 \gtrsim \frac{\epsilon^{4/3} M^2}{3(2\pi)^4 \alpha'^2} \int_0^{\eta_{UV}} I(\eta) \sinh^2 \eta d\eta \quad (2.10)$$

obtained by performing a dimensional reduction and integrating out the Einstein action over the internal manifold, [44].

It is worth pausing to emphasize the geometrical consequences of this throat geometry, as these feed into the string equations of motion. The prefactor h is very sharply peaked at the base of the throat, and thus leads to a large hierarchy between our four-dimensional noncompact physics and the underlying ten-dimensional scales. For example, if we consider a length scale, such as the string effective width w_4 in our universe, then near the tip this is equivalent to an internal range of η given by $w_4^2 \sim (g_s M \alpha')^2 \epsilon^{-4/3} (\delta\eta)^2$, or

$$w_4^2 M_p^2 \gtrsim \frac{\alpha' g_s^2 M^4}{3(2\pi)^4} \epsilon^{-4/3} (\delta\eta)^2 \quad (2.11)$$

(using (2.10), and replacing the integral with an estimate in terms of $r_{UV}^2 = \mathcal{O}(\alpha')$). For the string width scale, we expect $w_4^2 M_p^2 \simeq 1/(G\mu) \sim 10^7 - 10^{12}$, and for typical compactification data considered in brane inflation models (see [45] for a translation of this to the KS parameters used here) the prefactor on the RHS of (2.11) is $10^{12} - 10^{14}$, hence $(\delta\eta)^2$ is likely to be extremely small.

To get the equations of motion, we therefore take the zero width classical string effective action, [13, 14], i.e. the Nambu action (1.1). Because our metric is nontrivial, we cannot take the usual temporal conformal gauge used by Kibble and Turok, [28], in which the induced metric on the string worldsheet is conformally flat with worldsheet and bulk time identified, and in which the motion of the string reduces to left and right moving uncoupled waves. Instead, we choose the transverse temporal gauge: $\sigma^0 = X^0 \equiv t$, $\dot{X}^a X'_a = 0$. This identifies worldsheet time with background time and imposes diagonality on the worldsheet metric $\gamma_{AB} = X_{,A}^a X_{,B}^b G_{ab}$. Variation of the

Nambu action gives a wave equation for X^a :

$$\square X^a + \Gamma_{bc}^a X^b_{,B} X^c_{,C} \gamma^{BC} = 0 \quad \Rightarrow$$

$$\frac{\partial}{\partial t} \left(\frac{\dot{X}^a X'^2}{\sqrt{-\gamma}} \right) + \frac{\partial}{\partial \sigma} \left(\frac{X'^a \dot{X}^2}{\sqrt{-\gamma}} \right) + \frac{1}{\sqrt{-\gamma}} \Gamma_{bc}^a \left(X'^2 \dot{X}^b \dot{X}^c + \dot{X}^2 X'^b X'^c \right) = 0, \quad (2.12)$$

where a dot denotes differentiation with respect to time and prime the spacelike worldsheet coordinate $\sigma^1 \equiv \sigma$.

It is now straightforward to see why the conformal gauge cannot be simultaneously chosen with the synchronous gauge, even if our four-dimensional universe is flat, by examining the $a = 0$ equation which reduces to

$$\frac{\partial}{\partial t} \left(\sqrt{\frac{-X'^2}{h \dot{X}^2}} \right) = 0 \quad (2.13)$$

for the case $g_{\mu\nu} = \eta_{\mu\nu}$. Clearly, if h varies significantly over the timescales of interest, then the synchronous gauge will not be a good approximation.

In order to explore the range of string motion, we first look at some simple trajectories in a background where the non-compact dimensions are flat, before considering how to extract more general trajectories and to include more physics such as cosmological expansion and gravitational backreaction.

3. String motion in a static spacetime

We first consider strings in a Minkowski background, $g_{\mu\nu} = \eta_{\mu\nu}$ in order to derive the basic behaviour of a loop. If the full spacetime is flat, then the Kibble-Turok, [28], method for building general solutions can be applied. In the warped background however, this is no longer the case, and we must look carefully at how the internal and external directions interact through the warp factor. It is useful to first consider a simple trajectory to explore the main issues associated with warping, thus we restrict the internal motion to only two directions, looking at movement in the radial η -direction and one angular direction. In order that the angular motion is a stable trajectory (i.e. that it does not induce motion in any of the other angular directions) we must take it to be along a great circle within the conifold, and in particular avoiding any coordinate singularities, such as polar singularities. We explicitly choose $\theta_1 = \theta_2 = \frac{\pi}{2}$, $\psi = \pi$, $\phi_1 = \phi_2 = \phi$, thus having the string move around the non-contractible S^3 , which is a consistent angular trajectory. The metric effectively becomes:

$$ds^2 = h^{-1/2} (dt^2 - d\mathbf{x}^2) - h^{1/2} \epsilon^{\frac{4}{3}} \left[\frac{d\eta^2}{6K^2(\eta)} + B(\eta) d\phi^2 \right], \quad (3.1)$$

where $B(\eta) = K(\eta) \cosh^2(\frac{\eta}{2})$. By modelling the motion of string loops in this spacetime, we hope to capture essential aspects of their dynamics in the full 10D

spacetime. The string worldsheet can be written as:

$$X^a(t, \sigma) = (t, \mathbf{x}(t, \sigma), \eta(t, \sigma), \phi(t, \sigma)). \quad (3.2)$$

Substituting this into the equation of motion, (2.12), gives the explicit set of equations for the spacetime coordinates of the string worldsheet:

$$\ddot{\mathbf{x}} = \frac{1}{E} \left(\frac{\mathbf{x}'}{Eh} \right)' \quad (3.3)$$

$$\begin{aligned} \ddot{\eta} = & \frac{1}{E} \left(\frac{\eta'}{Eh} \right)' + \frac{h_{,\eta}}{E^2 h^2} \left(\frac{3K^2}{\epsilon^{4/3} h} \dot{\mathbf{x}}'^2 + \eta'^2 \right) + \dot{\eta}^2 \left(\frac{K_{,\eta}}{K} - \frac{h_{,\eta}}{2h} \right) \\ & - \frac{K_{,\eta}}{K} \frac{\eta'^2}{E^2 h} + \frac{3K^2}{h} \left[(Bh)_{,\eta} \dot{\phi}^2 - B_{,\eta} \frac{\phi'^2}{E^2} \right] \end{aligned} \quad (3.4)$$

$$\ddot{\phi} = \frac{1}{E} \left(\frac{\phi'}{Eh} \right)' + \left(\frac{h_{,\eta}}{h} + \frac{B_{,\eta}}{B} \right) \left(\frac{\phi' \eta'}{E^2 h} - \dot{\phi} \dot{\eta} \right). \quad (3.5)$$

The quantity E that appears in these equations is given by:

$$E = \sqrt{\frac{-X'^2}{h\dot{X}^2}} = \sqrt{\frac{\mathbf{x}'^2 + h\epsilon^{\frac{4}{3}} \left(\frac{\eta'^2}{6K^2} + B\phi'^2 \right)}{h \left(1 - \dot{\mathbf{x}}^2 - h\epsilon^{\frac{4}{3}} \left(\frac{\dot{\eta}^2}{6K^2} + B\dot{\phi}^2 \right) \right)}. \quad (3.6)$$

From the equation of motion for t , (2.13), we have $\dot{E} = 0$, i.e. E is a conserved quantity. It is related to the conserved energy of the system, \mathcal{E} , by:

$$\mathcal{E} = \mu \int E(\sigma) d\sigma. \quad (3.7)$$

Given that E is conserved, it is easy to draw some qualitative conclusions from (3.6). Essentially, the numerator in (3.6) is related to the length of the string (via integration) and the denominator (ignoring h) how relativistic the string is at a particular time. As the string falls down the throat, h increases sharply, thus presuming the string is not highly relativistic all along its length, the X'^2 term must increase to compensate. Thus a string falling down the throat will grow in the noncompact directions, as well as stretching out in the internal directions, and vice versa. However, there is clearly no friction term in these equations of motion to cause the string to fall and be confined at the tip of the throat; rather, it is free to ‘bounce’ back up again. We will see this in both a simple example, as well as a full integration.

In flat spacetime, it is easy to obtain analytic solutions to the equations of motion [28]. In warped spacetime, however, the equations of motion (3.3)-(3.5), which are partial differential equations in t and σ , are coupled and non-linear, and it is very difficult to find an analytic solution. One exception to this is the rather special case in which the string is precisely at $\eta = 0$: the tip of the throat. Here, motion along a single great circle is now exactly of the form considered in [39, 40], where the

extra dimension is circular. Strings at the tip of the conifold have been considered in [46], although the trajectory considered there is rather special as it occurs at a polar singularity and actually corresponds to a circular loop boosted along its length to the speed of light. However, in spite of being somewhat non-generic, angular motion of the string at the bottom of the conifold can give interesting consequences for the noncompact trajectories, [47].

In order to model the dynamics we first look at a simple loop trajectory that reduces the partial differential equations to ordinary differential equations. We then go on to deduce general properties of string motion from the conserved energy, and to plot numerical solutions to the full equations of motion.

3.1 A simple Ansatz

A simple set-up in which the loop is pointlike in the internal dimensions and circular in the external dimensions reduces the equations of motion to a set of ordinary differential equations in t . The string has the freedom to move around in the throat, and for its radius in the external dimensions to expand and contract. We parametrize it as follows:

$$x^M = (t, \rho(t) \cos \sigma, \rho(t) \sin \sigma, 0, \eta(t), \phi(t)) , \quad (3.8)$$

where $\rho(t)$ is the radius of the loop in the external dimensions, and the internal coordinates, $\eta(t)$ and $\phi(t)$, depend only on time.

The time-independent quantity E , given by equation (3.6), is now also independent of the spacelike worldsheet coordinate, σ , so it is an absolute constant:

$$E = \sqrt{\frac{\rho^2}{h \left(1 - \dot{\rho}^2 - h \epsilon^{\frac{4}{3}} \left(\frac{\dot{\eta}^2}{6K^2} + B \dot{\phi}^2 \right) \right)}} = E_0 \quad (3.9)$$

The equations of motion for ρ and η become:

$$\ddot{\rho} = -\frac{\rho}{E_0^2 h} \quad (3.10)$$

$$\ddot{\eta} = \frac{3K^2 h_{,\eta} \rho^2}{\epsilon^{\frac{4}{3}} E_0^2 h^3} + \dot{\eta}^2 \left(-\frac{1}{2} \frac{h_{,\eta}}{h} + \frac{K_{,\eta}}{K} \right) + 3K^2 \dot{\phi}^2 \left(\frac{h_{,\eta}}{h} B + B_{,\eta} \right) . \quad (3.11)$$

There is now a conserved angular momentum in the throat:

$$J = \dot{\phi} h B = \text{const.} \quad (3.12)$$

This is a Hamiltonian system with the conserved quantity E_0 being the Hamiltonian. Rearranging (3.9), using (3.12), expresses the system as motion in an effective potential:

$$\dot{\rho}^2 + \dot{R}^2 = 1 - \frac{\rho^2}{E_0^2 h} - \frac{\epsilon^{\frac{4}{3}} J^2}{h B} = 1 - V_{\text{eff}}(\rho, R) , \quad (3.13)$$

where

$$dR = \sqrt{\frac{h}{6}} \frac{\epsilon^{\frac{2}{3}} d\eta}{K} \quad (3.14)$$

is an alternative conformal radial coordinate. In this system, since E is conserved, we have free motion with no energy being lost¹.

We can now qualitatively see the effect of motion in the throat from the form of this potential. First note that $E_0^2 h$ sets the scale of oscillations in ρ , thus as the string moves down the throat, the overall size of the string in the noncompact directions will increase as already noted. Therefore a string moving down from the UV will dump energy into our visible loop. However, it is clear from the form of the equations of motion that that energy will not remain in our noncompact dimensions, but that the string will continue to move back up the throat leeching energy back, and continuing to oscillate. The timescales of these relative oscillations depend on the initial scale of ρ , and the compactification parameters.

To get an estimate of motion (before presenting some exact solutions), consider a very simple set-up. Suppose that the loop has only radial motion in the throat, and is very close to the tip (i.e. the energetically favoured potential minimum), then expanding the various functions in the metric near the tip, we obtain

$$V_{\text{eff}}(\rho, R) = \frac{\epsilon^{8/3}}{2E_0^2 (g_s M \alpha')^2 I_0} \frac{\rho^2}{I_0} \left(1 + \frac{\epsilon^{4/3}}{3(g_s M \alpha')^2} \frac{R^2}{I_0^2} \right) \quad (3.15)$$

where $I_0 = I(0) = 0.5699$ is the value of the integral (2.3) at the tip of the throat. We can now see the hierarchy of scales: provided $R \ll g_s M \alpha' \epsilon^{-2/3}$, ρ will have harmonic motion at a frequency $\omega_\rho \sim \epsilon^{4/3} / (g_s M \alpha' E_0)$. Since the scale of ρ is set by the string length, L , which is of order the Hubble scale for current day cosmic strings, this frequency is of order L^{-1} , as might be expected for a cosmic string. However, superimposed on this general behaviour are oscillations in R , which have a frequency set by the compactification parameters: $\omega_R \sim \epsilon^{2/3} / (g_s M \alpha') \gg \omega_\rho$.

This is of course a ‘‘broad brush’’ behaviour, once ρ becomes very small, the timescale of motion in R lengthens, and R can potentially move further up the throat. In fact, there is no reason in principle for the motion not to explore all regions of the effective potential. As this is a Hamiltonian system, it does not have attractors (regions to which trajectories converge over time), and therefore there is no mechanism by which a string could be completely confined at the tip of the throat. Indeed, for small J , the potential is strongly ‘creased’ at $\rho = 0$, with a sharp valley along the R -direction. This makes the motion very sensitive to initial conditions should the loop happen to hit this direction in phase space. We see this in some of numerical integrations.

¹In reality, of course, the string will be losing some energy, for example through gravitational radiation, which we model in section 4.2.

The picture with angular momentum is broadly similar, as unless J is improbably large, the term in (3.13) is generally small. The main qualitative difference with angular momentum is that it gives a hard bound on how far up the throat the string can move, since

$$\frac{\epsilon^{\frac{4}{3}} J^2}{h(\eta)B(\eta)} \leq 1. \quad (3.16)$$

It is straightforward to solve these equations of motion numerically, although for practical reasons, we cannot access the most physically realistic huge hierarchies between the scale of the throat and the current cosmological cosmic string network scale. However, these solutions can test the general understanding built up by analysing the system as above. Figure 1 shows a demonstration of the qualitative motion described above. Here, the rather improbable set of data has been chosen: $\epsilon = 0.1\alpha'^{3/4}$, $g_s M = 100$, $\rho(0) = 10^4\sqrt{\alpha'}$, $\eta(0) = 0.25$ (implying $R(0) = 57.86\sqrt{\alpha'}$). For vanishing angular momentum these give the values $E_0 = 4.4$, $\omega_\rho = 1.1 \times 10^{-4}$, $\omega_R = 2.2 \times 10^{-3}$. While these values are clearly small, they are obviously highly unrealistic, nonetheless, the behaviour of the loop does broadly follow the description given above. In the external dimension the loop oscillates with approximately the above frequency ω_ρ , while in the throat the loop oscillates faster, and when ρ becomes small, it ‘coasts’, since the potential (3.15) is effectively flat. Note how this behaviour leads to the loop moving occasionally further up the throat, where the above approximation to the potential will break down – even so, the broad brush behaviour continues, although the internal oscillations seem to prefer being stronger than the initial conditions would suggest.

One can see on figure 1 the exchange of energy between the two sectors, since when internal oscillations of the loop are larger, external ones are smaller, and vice versa. Figure 2 shows that a similar exchange occurs in the velocities. Clearly, the internal velocity, v_η , becomes small when external velocity, v_ρ , is large (which corresponds to the radius passing through zero). Looking more closely, one can see that, in agreement with [41] for open strings, the 3D velocity is modulated by the high frequency internal oscillations.

The presence of an internal velocity is the important feature that in [39, 40] was found to make a remarkable difference to the gravitational wave signal given off by string loops. The internal velocity causes the cusps on the string motion to be rounded off, and also to be less likely to form. This effect was measured by a “near cusp event” parameter $\Delta \simeq \sqrt{1 - \dot{\mathbf{x}}^2}/2$, which we can compute by finding local maxima of the external velocity, $|\dot{\mathbf{x}}|$, for these simple trajectories. For the loops plotted in figure 1, we find that $\langle \Delta \rangle = 0.071, 0.059, 0.099$, and 0.252 for $J = 0, 5\%, 10\%$, and 50% of J_{\max} respectively. The large value of $\langle \Delta \rangle$ for large J is not surprising: in this case the loop has, by construction, a (conserved) relativistic internal motion. The values of $\langle \Delta \rangle$ for small, or zero, J are more relevant, as these represent initial conditions where there is little relativistic motion internally. Exploring further the

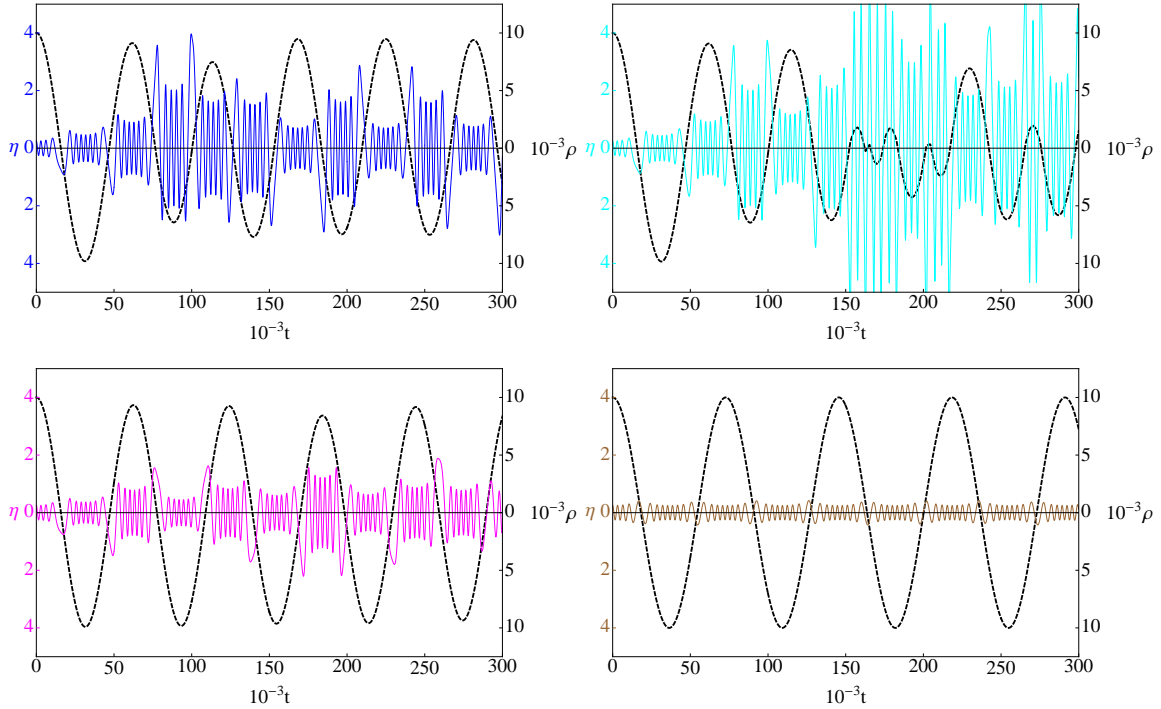


Figure 1: Numerical solutions for the circular loop Ansatz (3.8) showing the internal location $\eta(t)$ (in colours) and the external radius $\rho(t)$ (in dashed black) of the loop, demonstrating the interplay between external and internal motion and the effect of angular momentum in the internal dimensions. The plots show a loop of size $\rho_0 = 10^4 \sqrt{\alpha'}$ initially starting at rest at $\eta_0 = 0.25$, with $J = 0, 5, 10$, and 50% of the relativistic maximum $\epsilon^{-2/3} \sqrt{h(\eta_0) B(\eta_0)}$, with $\eta(t)$ shown in blue, cyan, magenta, and brown respectively. In all plots, the external loop radius, ρ , is shown in dashed black.

parameter space for $J = 0$ yields $\langle \Delta \rangle = 0.012, 0.048$, and 0.035 for initial loop radii of $20\text{K}\sqrt{\alpha'}$, $30\text{K}\sqrt{\alpha'}$ and $40\text{K}\sqrt{\alpha'}$ respectively, indicating that this is not a parameter which drops as the loop size is increased, but rather seems to respond more to the interplay between the internal and external dimensions.

We conclude that in the presence of a warped throat, this particular loop trajectory has significant internal motion and cannot be approximated as effectively 4D.

3.2 More general loops

A general shape of loop will have much more complicated motion than the simple oscillations modelled in the previous section. There are potential terms in the equation of motion for η , equation (3.4), that include the derivative of the warp factor,

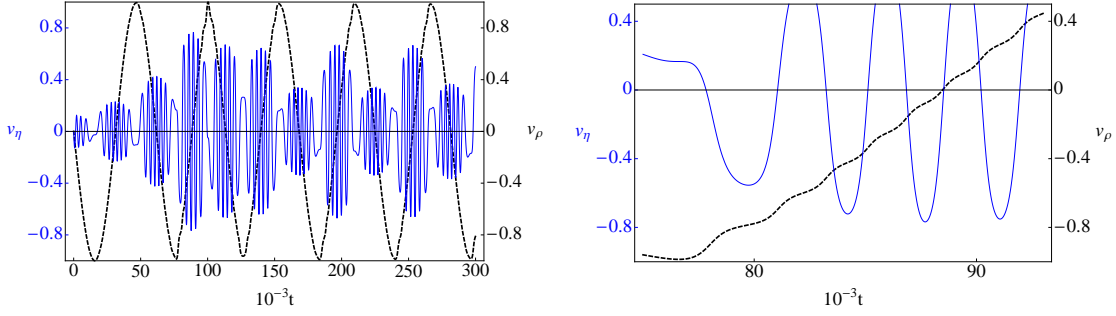


Figure 2: Left: The physical velocities, v_η (blue) and v_ρ (dashed black), corresponding to the first plot of figure 1 ($J = 0$). It is clear that energy is transferred back and forth between the two. Right: Detail from the left hand plot showing modulation of the 3D velocity, v_ρ (dashed black), due to the higher frequency internal oscillations.

h , for example the second term:

$$\frac{h_{,\eta}}{h} \frac{1}{E^2 h} \left(\frac{3K^2}{\epsilon^{\frac{4}{3}} h} \mathbf{x}'^2 + \eta'^2 \right). \quad (3.17)$$

Terms like this have the opposite sign to η and therefore induce oscillations of the string up and down the throat. However, intuitively one expects the string's own tension to pull different parts of it in different directions, which, coupled with the forces from the warped throat, will result in complicated dynamics.

If, for a moment, we assume that the loop is very close to the tip of the throat, we can do a similar expansion to that of (3.15) for a more general loop. If we first make the transformation $\sigma \rightarrow \tilde{\sigma}$ such that $d\tilde{\sigma} = E(\sigma)d\sigma$, then $\tilde{\sigma}$ runs from 0 to L , the (10D) length of the loop, and the equation of motion for the external part of the loop (3.3) becomes:

$$\ddot{\mathbf{x}} = \frac{1}{h} \left(\mathbf{x}'' - \frac{\mathbf{x}' h_{,\eta} \eta'}{h} \right) \quad (3.18)$$

where prime is now differentiation with respect to $\tilde{\sigma}$.

If we assume the external part of the loop is of cosmological size, it will contain most of the length of the string, i.e. $|\mathbf{x}| \sim \mathcal{O}(L)$. Then, assuming the loop can be approximated by low harmonics only, we also have

$$|\mathbf{x}'| \sim \mathcal{O}(1) \quad ; \quad |\mathbf{x}''| \sim \mathcal{O}\left(\frac{1}{L}\right) \quad ; \quad \eta' \sim \mathcal{O}\left(\frac{\eta}{L}\right). \quad (3.19)$$

Expanding h and $h_{,\eta}$ in small η gives the following:

$$h \simeq (g_s M \alpha')^2 \epsilon^{-\frac{8}{3}} \left(\frac{2}{3}\right)^{\frac{1}{3}} \left(0.72 - \frac{\eta^2}{3}\right) \quad ; \quad \frac{h_{,\eta}}{h} \sim \eta. \quad (3.20)$$

This implies that $\frac{h_{,\eta} \eta'}{h} \sim \frac{\eta^2}{L}$, and thus that the second term on the RHS of (3.18) is $\mathcal{O}(\eta^2)$ suppressed relative to the first. Thus if $\eta \ll 1$, or $R \ll g_s M \alpha' \epsilon^{-2/3}$, the overall

factor of $\frac{1}{h}$ is approximately constant, and motion will be close to a Kibble-Turok solution, for which left and right-moving modes are independent, i.e. the effect of the internal motion will be small. Indeed, the form of this correction suggests that corrections to the Kibble-Turok motion will be (roughly) of order $\mathcal{O}(\eta^2)$. Returning to our simple solutions of figure 1, computed with initial data $\eta_0 = 0.25$, this would suggest a discrepancy of order 0.04 from the exact 4D Nambu string, which is the ballpark of the estimates for Δ from the numerical solutions.

For a loop solution of the type (3.2) with significant and generic motion in the internal dimensions, however, a numerical integration of the PDE's (3.3-3.5) is necessary to find the detailed and explicit trajectory. To explore the effect of more complex internal motion, we started with a circular loop in the external space, as in the simple Ansatz in the previous section, but instead of the ‘‘pointlike’’ internal motion of our previous Ansatz, we allowed for a loop structure in the internal dimensions as well. Note, that even though the initial loops (both in the external and internal dimensions) were set up to be circular, there is now no symmetry condition imposed on the solution at $t > 0$. Figures 3 and 4 show some sample snapshots of the loop’s motion once the evolution is underway. In these plots, for numerical expedience the more unrealistic compactification parameters, $g_s M = 10$ and $\epsilon = 0.5\alpha'^{3/4}$ were used, and the radii of the internal and external extent are more similar.

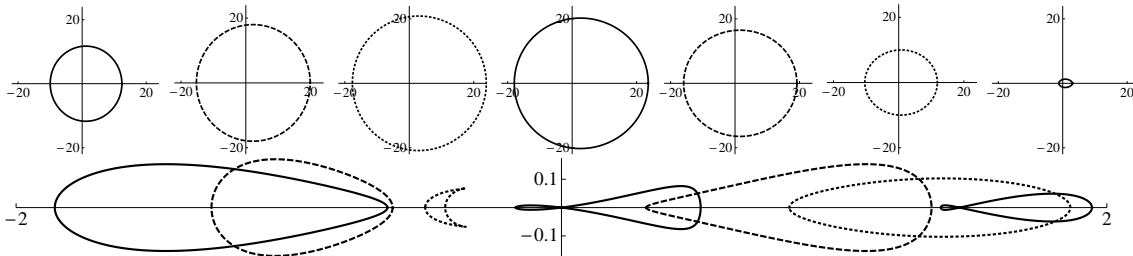


Figure 3: Snapshots of a string loop evolving both externally (upper) and internally (lower), where the initial internal loop is displaced up the throat. In the lower plot, the axes are $\eta \cos \theta$ and $\eta \sin \theta$, and the snapshots are selected some time after the start of the integration.

The plots show how, broadly, the features that were demonstrated in the simple Ansatz are also present here: the loop oscillates up and down the throat with periods when motion is concentrated closer to the tip translating into a larger, or more relativistic, loop in the external dimensions (and vice versa). Figure 3 shows an example with the loop starting up the throat, moving down and back up again, while also changing shape under its own tension. Although the loop is clearly no longer pointlike in the internal dimensions, it is fairly localised, making the trajectory close to that of the simple ansatz. Indeed a similar behaviour is seen to occur, with the external part of the loop remaining roughly circular and oscillating in and out, its maximum radius of oscillation depending on how close to the tip of the throat the

loop is at the time (which we see by observing the trajectory over longer timescales). A fairly coherent oscillation of the whole loop up and down the throat is also observed. This consistency of the full system with the simple ansatz reinforces the conclusions made in section 3.1. Notably, on figure 3, the loop becomes larger as the internal loop contracts. Although in a realistic cosmological setting, there would be a large hierarchy between internal and external frequencies, we would still expect to see a similar exchange of energy (as in figure 1, for example), averaged over internal oscillations.

Figure 4 focuses instead on a loop whose initial internal configuration encircles the origin, and has a significant variation in η . Here, the part of the loop at larger η starts to fall down the throat, whereas the part at lower η begins to move up. As the loop then has varying motion internally, this feeds into the external motion, causing the loop there to start curling, forming (apparently) a double loop, then a very wrinkled loop. This particular example shows a dramatic change of shape in the external dimensions, which we expect will be muted as the radius of the loop in the external dimensions is increased to more realistic cosmological scales.

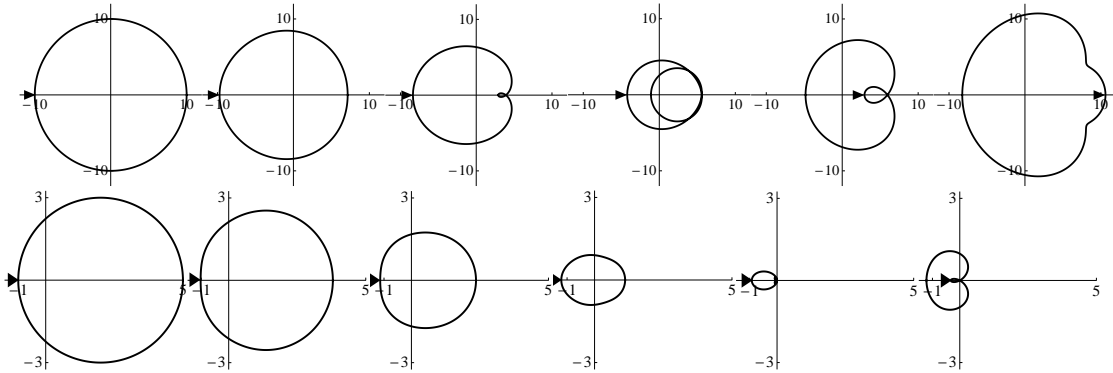


Figure 4: From left to right, snapshots of a string loop at evenly spaced time intervals, the upper sequence showing the loop in the external dimensions, and the lower sequence in the internal dimensions. This solution demonstrates how the circular shape is distorted by internal motion, and develops apparent kinks and crossings (although the loop does not self intersect as it misses in the internal dimensions). The arrow denotes the position on the loop where $\sigma = 0$ for comparison of the location of the features.

It is interesting to note that even for a finite energy, \mathcal{E} , there is no hard bound on how far from the tip of the throat a string can move (i.e. how large η can be). While we can bound the variation in η at a particular time ($\mathcal{E} \geq \mu\epsilon^{2/3} \int d\sigma |\eta'| / \sqrt{6}K = 2\mu\epsilon^{2/3} \Delta R(t)$), we can nonetheless have the loop high up the throat if we effectively ‘freeze’ it in the external dimensions (i.e. temporarily have the loop very small and nonrelativistic). Such a situation however, would require a conspiracy of internal and external motion that makes it unlikely, or a rare event. More generically, we expect a loop to approximately remain within an order of magnitude or so of its

initial data (in the absence of cosmological evolution) as it is unlikely for a loop with general internal shape to move significantly up the throat. Even this however, is enough to maintain sufficient internal motion, and does not preclude significant local alterations, such as the quirks exhibited in figure 4.

3.3 Effect of two-form charges

In many explorations of cosmic superstrings, the strings are considered to interact with the IIB supergravity fields, in particular the NS-NS 2-form (for the fundamental string) or the RR 2-form (for the D-string), or indeed both (for (p, q) strings). While it is unclear to what extent these supergravity interactions remain at low energies, since the exact solution we are using for the throat contains fluxes of both these fields, we should be mindful of the effect of these 2-forms on the motion of the strings. A fully general solution will be rather involved, however, we comment here on general features of including these terms in the motion of the string. For a string charged under a 2-form, the Nambu action acquires an additional term:

$$S \propto - \int d\sigma dt \sqrt{-\gamma} + \int d\sigma dt \epsilon^{AB} X_{,A}^a X_{,B}^b B_{ab}. \quad (3.21)$$

The equation of motion is then:

$$\frac{1}{\sqrt{-\gamma}} \left[\frac{\partial}{\partial t} \left(\frac{\dot{X}^a X'^2}{\sqrt{-\gamma}} \right) + \frac{\partial}{\partial \sigma} \left(\frac{X'^a \dot{X}^2}{\sqrt{-\gamma}} \right) \right] + \frac{1}{\gamma} \Gamma_{bc}^a \left(X'^2 \dot{X}^b \dot{X}^c + \dot{X}^2 X'^b X'^c \right) \quad (3.22)$$

$$= (\dot{X}^b X'^c - X'^b \dot{X}^c) H_{bc}^a.$$

Here we will consider explicitly $H_3 = dB_2$ from the 2-form (2.8), as this will capture the essential qualities of including charge in the string. (A D-string couples differently to the fluxes, but the impact will be qualitatively the same.)

The key feature of including charge for the string is that, just like the path of a charged particle is curved in a magnetic field, the charged string will pick up transverse forces coming from the H_3 or F_3 fluxes. Thus, we do not expect a simple single-angle motion, such as that of the simple Ansatz considered in (3.2). In fact, if one sets $\theta_1 = \theta_2 = \pi/2 = -\psi/2$, and $\phi_1 = \phi_2 = \phi(t, \sigma)$, then we have a nonzero ‘force’ in the θ_i directions given by

$$F^{\theta_1} = -F^{\theta_2} = 4g_s M \epsilon^{-4/3} \frac{k'(\eta)}{\sqrt{h} B(\eta)} (\dot{\eta} \phi' - \eta' \dot{\phi}), \quad (3.23)$$

where $k'(\eta)$ is the derivative of the function premultiplying $g^3 \wedge g^4$ appearing in (2.8). This shows that the general motion will be quite involved. However, clearly at least one internal coordinate must have σ dependence as well as time dependence in order for this effect to show up, so in fact the simple time dependent only Ansatz used in Section 3.1 is still a valid solution.

Since there is no H^0_{ab} component, the quantity E given by the Nambu dynamics is still conserved, so the system still has a conserved energy. In order for the B-field to localise the string at the bottom of the throat, therefore, energy would have to be transferred into the other dimensions. This would require a damping term in the equation of motion for η , ie. a term with opposite sign to $\dot{\eta}$. The extra terms in the equation of motion for η that are induced by the B-field are (from (3.22)):

$$(\dot{X}^b X^{tc} - X^{tb} \dot{X}^c) g^{\eta m} H_{\eta bc}. \quad (3.24)$$

Since H_3 is antisymmetric, both b and c must be angular directions, so there can be no term containing $\dot{\eta}$, and therefore no damping term.

One interesting piece of information that can explicitly be extracted from the B-field is the behaviour at the tip of the throat. In the case of purely Nambu dynamics, if a string is placed at rest at the tip of the throat, the Nambu equation of motion for η (the radial coordinate) will vanish and it will simply stay there. Although one would not expect a general trajectory to reach this configuration, it is a valid solution. In the presence of the B-field, however, this is no longer the case. This stems mainly from the fact that part of the conifold geometry does not shrink to zero size at the tip of the throat, so it is still possible to have angular dependence and motion. In fact the geometry at the tip of the throat is a round 3-sphere, which can be parametrized by setting $\theta_1 = \phi_1 = 0$, so the coordinates on the S^3 are θ_2 , ϕ_2 and ψ .

By calculating the relevant terms in H_3 , we find that the following non-zero term appears in the equation of motion for η at $\eta = 0$:

$$\left(\phi'_2 \dot{\theta}_2 - \dot{\phi}_2 \theta'_2\right) h^{\frac{1}{2}}(0) \epsilon^{-\frac{4}{3}} (g_s M \alpha') K^2(0) \sin \theta_2 \sim \left(\phi'_2 \dot{\theta}_2 - \dot{\phi}_2 \theta'_2\right) \sin \theta_2.$$

Thus, if a string has both non-trivial extent and velocity on the 3-sphere, the presence of the B-field provides a force in the η direction and pushes the string away from the origin, which further supports our argument that it will, in general, not be localised there.

Finally, since the interaction with fluxes clearly increases the amount of internal motion, the effect on the external loop motion will be to make it deviate even more from the exact Kibble-Turok form.

4. Cosmological loops

We have argued that the motion of loops in the presence of warped extra dimensions will include all dimensions, and will not be localised at the tip of the throat. This was based on the assumption of classical dynamics in a static spacetime. Potentially significant modifications to this behaviour come from a variety of factors. In the Nambu equations of motion we saw potential terms that caused the string to oscillate

about the tip of the warped throat, but argued that for it to be confined at the bottom, it would have to lose energy in the internal dimensions, which would require some kind of friction. Cosmological expansion causes damping of long strings in a network [48, 49], and therefore may provide this internal friction. Energy loss via emission of gravitational radiation must also be considered, since if a string were to lose more energy in the internal dimensions than the external ones this could result in an effectively 4D motion. We now consider both of these effects and find that our conclusions remain unchanged.

4.1 Cosmological expansion

In an expanding universe, the velocities of long strings are damped, allowing the network to reach a scaling solution [48, 49]. Thus cosmological expansion might prove to be a source of damping in the internal dimensions, which might result in strings being confined to the bottom of the warped throat. The important quantity to consider is the relative magnitude of internal and external damping, since a stronger damping in the internal dimensions would result in internal motion being effectively brought to a standstill, whilst the external part of the loop would continue to evolve, giving an effectively 4D motion. In [41], this was explored for long strings, and it was found that internal damping is in fact very weak, and does not localise the strings at the tip of the throat.

The effect of expansion on closed loops is more interesting. While outside the horizon scale, they behave similarly to long strings: expansion effectively has a “stretching” effect, and reduces the velocity of the string. For the closed loop, stretching increases its total energy, and does slow down the motion of the loop for a while, but eventually the tension of the loop causes it to contract and fall inside the horizon. Once the loop is well inside the horizon, expansion ceases to affect its motion. The transition between these two stages, when the loop is comparable to the horizon size, can have interesting dynamics.

For an FRW universe, the metric now takes the form:

$$ds^2 = h^{-\frac{1}{2}}(dt^2 - a^2 d\mathbf{x}^2) - h^{\frac{1}{2}} \tilde{g}_{mn} dy^m dy^n, \quad (4.1)$$

so that the physical distance in the external dimensions is now $a\mathbf{x}$. The scale factor, a , can be taken to be proportional to t^β , where $\beta = \frac{1}{2}, \frac{2}{3}$ respectively in the radiation and matter eras. The scalar $E \equiv \sqrt{\frac{-X'^2}{h\dot{X}^2}}$, which in flat spacetime was conserved, now depends explicitly on the scale factor $a = a(t)$:

$$E = \sqrt{\frac{a^2 \mathbf{x}'^2 + h\epsilon^{\frac{4}{3}} \left(\frac{\eta'^2}{6K^2} + B\phi'^2 \right)}{h \left(1 - a^2 \dot{\mathbf{x}}^2 - h\epsilon^{\frac{4}{3}} \left(\frac{\dot{\eta}^2}{6K^2} + B\dot{\phi}^2 \right) \right)}}. \quad (4.2)$$

The equations of motion become:

$$\dot{E} = -E \frac{\dot{a}}{a} \left(a^2 \dot{\mathbf{x}}^2 - \frac{a^2 \mathbf{x}'^2}{E^2 h} \right) \quad (4.3)$$

$$\ddot{\mathbf{x}} = \frac{1}{E} \left(\frac{\mathbf{x}'}{Eh} \right)' - \dot{\mathbf{x}} \frac{\dot{a}}{a} \left(2 - a^2 \dot{\mathbf{x}}^2 + \frac{a^2 \mathbf{x}'^2}{E^2 h} \right) \quad (4.4)$$

$$\begin{aligned} \ddot{\eta} = & \frac{1}{E} \left(\frac{\eta'}{Eh} \right)' + \frac{h_{,\eta}}{h} \frac{1}{E^2 h} \left(\frac{3K^2 a^2}{\epsilon^{\frac{4}{3}} h} \mathbf{x}'^2 + \eta'^2 \right) + \dot{\eta}^2 \left(\frac{K_{,\eta}}{K} - \frac{h_{,\eta}}{2h} \right) - \frac{K_{,\eta}}{K} \frac{\eta'^2}{E^2 h} \\ & + 3K^2 \dot{\phi}^2 \left(B_{,\eta} + \frac{h_{,\eta}}{h} B \right) - 3K^2 B_{,\eta} \frac{\phi'^2}{E^2 h} + \dot{\eta} \frac{\dot{a}}{a} \left(a^2 \dot{\mathbf{x}}^2 - \frac{a^2 \mathbf{x}'^2}{E^2 h} \right) \end{aligned} \quad (4.5)$$

$$\ddot{\phi} = \frac{1}{E} \left(\frac{\phi'}{Eh} \right)' + \left(\frac{h_{,\eta}}{h} + \frac{B_{,\eta}}{B} \right) \left(\frac{\phi' \eta'}{E^2 h} - \dot{\phi} \dot{\eta} \right) + \dot{\phi} \frac{\dot{a}}{a} \left(a^2 \dot{\mathbf{x}}^2 - \frac{a^2 \mathbf{x}'^2}{E^2 h} \right). \quad (4.6)$$

We see directly from (4.3) that the quantity E in (4.2), and therefore the total energy, $\mathcal{E} = \int d\sigma E$, is no longer conserved, as anticipated from its scale factor dependence. A straightforward consequence of (4.2) is that $-1 \leq \left(a^2 \dot{\mathbf{x}}^2 - \frac{a^2 \mathbf{x}'^2}{E^2 h} \right) \leq 1$, and hence

$$|\dot{E}| \leq E \frac{\dot{a}}{a}. \quad (4.7)$$

From this it follows that in order for \dot{E} to be significant, E must be a sizeable fraction of the horizon scale, i.e. $E \sim (\dot{a}/a)^{-1} = H^{-1}$. Physically, $\dot{E} \sim HE$ corresponds to a large, non-relativistic loop, where the energy is given by its rest-mass (length) and the dominant mechanism in (4.3) is conformal stretching, increasing the total energy. On the other hand, $\dot{E} \sim -HE$ corresponds to an ultra-relativistic loop, for which the relevant mechanism is velocity redshifting in the directions transverse to the string, decreasing the energy.

Useful insights into the behaviour of string loops in the spacetime (4.1) can be gained by focussing on the quantity E . Table 1 details extreme cases of string motion (i.e. cases in which the dynamics is dominated by certain types of terms), and the corresponding behaviour of E . We expect, and indeed find numerically, that energy is generally transferred back and forth between length and velocity (columns 1 and 2) and the extra dimensional motion (column 3). This implies that E can attain its limiting behaviour – increasing proportionally to the scale factor – only part of the time. In general, its growth will be slower, and, at certain intervals during the loop's evolution, E can even decrease. On the other hand, the scale factor, a , will always be increasing as t^β in a given era, and the horizon scale will grow even faster ($\propto t$). Thus, in finite time, E will no longer be a significant fraction of the horizon scale, \dot{E} will decrease, and E will return to being constant as in the case of non-expanding space. In other words, a large, horizon-scale loop is affected by expansion until it falls inside the horizon.

We see this behaviour in the simple Ansatz (3.8). Evolving numerically from such a circular configuration with superhorizon physical radius and zero velocities in

$\frac{a^2 \dot{\mathbf{x}}^2}{E^2 h}$	$a^2 \dot{\mathbf{x}}^2$	Internal velocity and length terms	E
large	small	small	$\propto a$
small	large	small	$\propto 1/a$
small	small	large	$\sim \text{constant}$

Table 1: Approximate behaviour of E when different length- and velocity-squared terms are dominant.

all dimensions, we see that that E begins by increasing proportionally to the scale factor, then oscillates up and down as the circular loop oscillates in and out, and approaches a constant value over time (Fig. 5). An interesting difference with respect to the pure 4D case becomes apparent. In 4D, a static, superhorizon loop starts with $\dot{E} \simeq (\dot{a}/a)E$ and this rate gets gradually reduced over cosmological timescales as the loop velocity slowly builds up from 0. Here, there is a second scale – that of the warping – which is hierarchically smaller than the expansion rate, and causes the build up of velocities in the compact dimensions over a much shorter timescale through the gradient terms in equation (4.5). As a result, the loop energy very quickly turns to a significantly slower expansion with $\dot{E} \sim (1/2)(\dot{a}/a)E$ (see Fig. 6), which can be understood from equation (4.3) with $a^2 \dot{\mathbf{x}}^2 \rightarrow 0$ and $h\epsilon^{\frac{4}{3}} \frac{\dot{\eta}^2}{6K^2} \lesssim 1^2$. Thus, the horizon, growing linearly in time, catches up with the physical loop size earlier than in 4D. Note, however, that a similar behaviour also occurs in 4D if the initial loop has small-scale-structure. In that case, the small-scale curvature generates velocity over short timescales and the situation is similar to the one we just discussed.

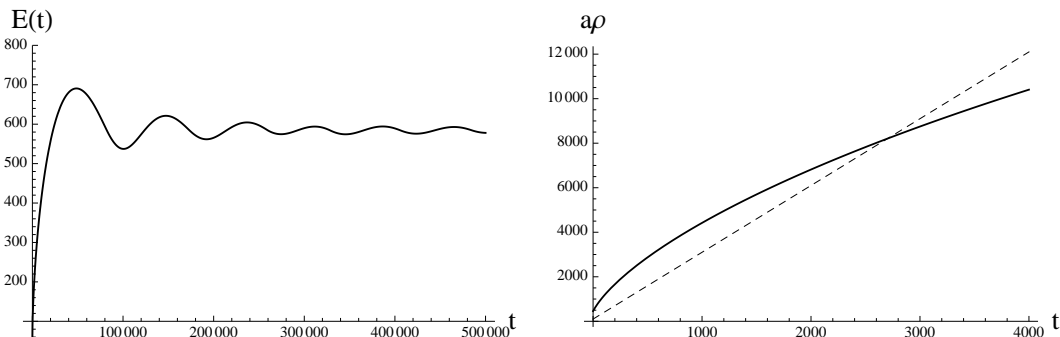


Figure 5: Left: Evolution of $E(t)$ for an initially static superhorizon loop. E is initially increasing but starts oscillating after the loop falls inside the horizon and eventually approaches a constant as in flat space. Right: Early evolution of the loop’s physical radius $a\rho$ (solid line) until it falls inside the horizon scale (dashed line). Over larger timescales (not shown), $a\rho$ undergoes oscillations with an amplitude that gets smaller with respect to the horizon, in accordance to the energy plot on the right.

²In fact, the velocity $h^{\frac{1}{2}}\epsilon^{\frac{2}{3}} \frac{\dot{\eta}}{\sqrt{6}K}$ oscillates in the interval $(-1, 1)$ and the rate \dot{E} changes accordingly on short timescales. Over larger timescales, the evolution can be approximated by taking the root-mean-squared velocity which is close to $1/2$.

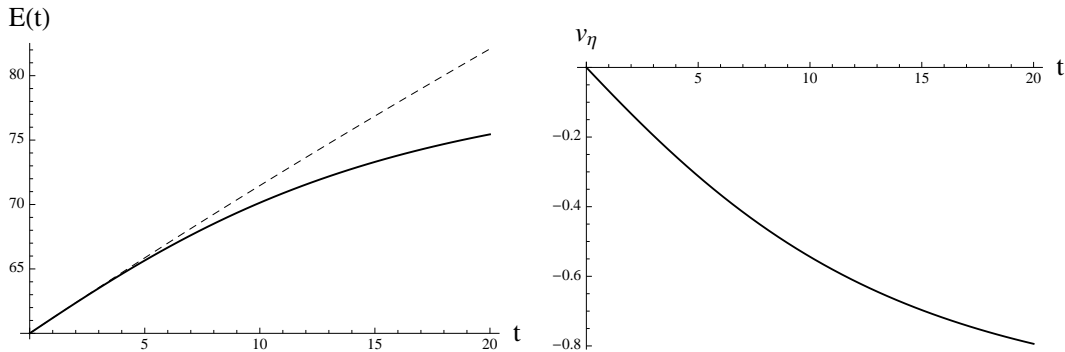


Figure 6: Left: Early time evolution starts as $E(t) \propto a(t)$ initially, but quickly drops to a slower rate as internal velocities (shown in the right plot) build up. The dashed line shows the $E(t) \propto a(t)$ growth, which would have been expected if there were no internal velocities. Right: Build up of internal velocity $v_\eta \equiv h\epsilon^{\frac{4}{3}} \frac{\dot{\eta}^2}{6K^2}$ over the same timescale, which, in view of equation (4.3), is responsible for the reduction of the rate \dot{E} in the left plot. Over larger timescales (not shown), v_η oscillates with $-1 \leq v_\eta \leq 1$ and the rate \dot{E} changes accordingly, so on much larger timescales the evolution can be approximated by taking the root-mean-squared $\langle v_\eta^2 \rangle \simeq 1/2$.

Having looked at the overall behaviour of E , we turn our attention to the Hubble terms proportional to $\frac{\dot{a}}{a}$ that appear in equations (4.4)-(4.6). Since these terms scale as $\frac{\dot{a}}{a} \propto \frac{1}{t}$ their relative effect generally becomes less important at later times, but they can still dominate during short intervals when the string radius crosses zero and E is kinetic energy-dominated. The term in the equation for external motion, (4.4), is a damping term, while the terms in the internal equations, (4.5) and (4.6), can in general have positive or negative sign with respect to the corresponding internal velocity.

It is important to note however, that although there is a damping term in the equation for \mathbf{x} , which reduces the size of its oscillations over time, the physical variable, $a\mathbf{x}$, does not get smaller. The damping term in equation (4.4) is stronger when the term $\frac{a^2 \dot{\mathbf{x}}^2}{E^2 h}$ is larger, corresponding to the loop radius being close to a local maximum. This implies that the comoving velocity, $\dot{\mathbf{x}}$, which is on average lowest in such configurations, will be slowed down even more in this region, so the string will tend to spend longer in such configurations. Then, looking back at the other equations, we see that this corresponds to the region where E is increasing and where the internal coordinates, η and ϕ , are being damped. This suggests that overall, the energy of a loop will slightly increase, and the extra dimensional motion will be slightly damped. The overall increase of energy is seen in the simple Ansatz, figure 5, and intuitively makes sense as the string is initially “stretched” by the expansion of space. The slight damping agrees with [41], but again it is not enough to localise the string. Then, after the loop falls inside the horizon, E becomes constant, and the string behaves exactly as it did in non-expanding space, as discussed above. Thus,

we confirm that Hubble damping alone cannot localise the strings in the internal dimensions. In fact, if E has increased from its starting value, motion in both sectors will be larger overall.

Figure 7 shows the evolution of the comoving radius ρ and the radial position η in the throat (left plot), together with the corresponding velocity evolutions (right plot), for the same loop considered above. Note that the apparent damping in the motion of the comoving radius is compensated by the scale factor growth $a(t) \propto t^\beta$, so overall the physical loop radius does not shrink at late times. (Here, we neglect gravitational radiation, to be studied in the next subsection 4.2.) As we have discussed, there is a small damping in the η motion, but the amplitude increases back again as energy is exchanged between the two sectors.

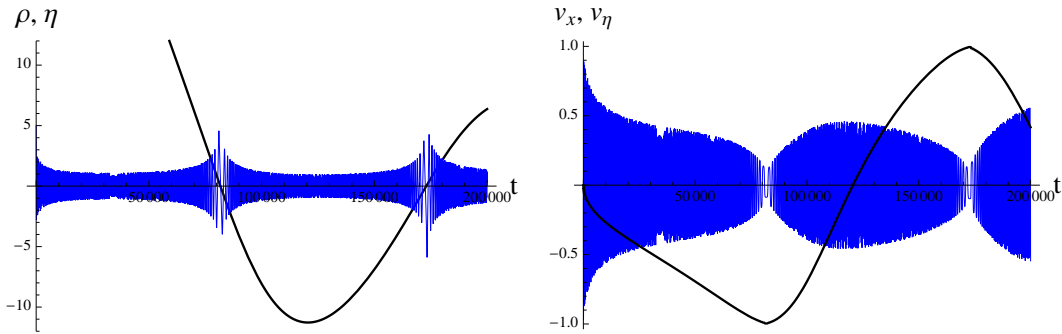


Figure 7: Left: Evolution of the comoving loop radius ρ (black thick line) and the internal radial coordinate η (blue thin line) for the initially superhorizon sized loop discussed above. The motion of η exhibits high-frequency oscillations up and down the throat, with an amplitude profile that is correlated with the 3D motion of ρ . The amplitude of η reaches a local maximum when ρ passes from 0, at which point **almost** all kinetic energy is in the 3D motion (cf. right plot). Right: Evolution of the physical velocities v_x (black thick line) and v_η (thin blue line) corresponding to ρ and η respectively. The internal velocity v_η oscillates at a much higher frequency, determined by the warping, becoming very small when the 3D velocity becomes relativistic, as the radius, ρ , passes through 0 (cf. left plot).

4.2 Gravitational radiation

Cosmic strings or superstrings lose energy via gravitational radiation, and while this is by no means the only form of radiation they produce, it is the most important for our purposes. For information on other forms of radiation, the emission of gamma rays, neutrinos and protons is discussed in [50]. However, this emission is only significant when loops are produced at the scale of the string width, and recent simulations [51] (but see also [52, 53, 54]) suggest that while there may initially be a high production of small loops, a scaling population of large loops at approximately $\frac{1}{20}$ of the horizon size becomes dominant, for which gravitational radiation is the main form of energy loss.

There has also been work recently on the emission of light from cosmic strings [55], but the power radiated by this mechanism is significantly smaller than that from gravitational radiation. In the context of string theory, cosmic (super)strings can emit many sorts of fields (for example [56] suggests that the Ramond-Ramond field would be the dominant form of radiation for cosmic D-strings) but these will only be produced at extremely high energies in the very early universe. Gravitational radiation will therefore be the dominant energy-loss mechanism for cosmic string loops for the majority of their history, so we chose to model this effect. Note, however, that other forms of radiation could be modelled in a similar way. Finally, note that the internal excitations on cosmic (super)strings could also be damped by their interaction with Kaluza-Klein (KK) gravitons [57]. However, over cosmological timescales such massive modes can be expected to decay, and we do not expect these to lead to an additional signal in the gravitational wave spectrum. While such a process can provide an additional damping mechanism, this will not qualitatively change any of our conclusions.

The emission of gravitational radiation by cosmic string loops can be approximated by a constant rate of decrease of the overall energy of the loop, until the energy reaches zero and the string has disappeared. In flat 4D spacetime, the following formula was derived by Vachaspati and Vilenkin [16] for the rate of energy loss from a loop:

$$\frac{d\mathcal{E}}{dt} \sim \Gamma G \mu^2, \quad (4.8)$$

where \mathcal{E} is the invariant energy of the loop (defined in (3.7)), μ the string tension and G is Newton's constant. Equation (4.8) is similar to the quadrupole formula that applies to slow-moving sources, with the addition of a numerical factor, Γ , which is usually evaluated to be approximately 50, [58]. This factor results from the fact that cosmic string loops are fast-moving, and, in particular, part of the contribution to Γ comes from cusps. As described in the introduction, these are events at which a point on the string instantaneously approaches the speed of light, and are generic on smooth loops in 4D. As discussed in [39, 40], allowing the string to move in extra dimensions greatly reduces the occurrence of cusps and may therefore affect the value of Γ . This would likely reduce the effective Γ , so taking $\Gamma \simeq 50$, could well be over-estimating the damping due to gravitational radiation.

The general behaviour, however, is independent of the numerical factor. The magnitude of the energy affects both how far away from the tip of the throat the string tends to move, and the maximum length of the loop. From (3.7) and (3.6),

the energy is:

$$\mathcal{E} = \mu \int d\sigma \sqrt{\frac{\mathbf{x}'^2 + h\epsilon^{\frac{4}{3}} \left(\frac{\eta'^2}{6K^2} + B\phi'^2 \right)}{h \left(1 - \dot{\mathbf{x}}^2 - h\epsilon^{\frac{4}{3}} \left(\frac{\dot{\eta}^2}{6K^2} + B\dot{\phi}^2 \right) \right)}} \geq \mu \int d\sigma \sqrt{\frac{\mathbf{x}'^2 + h\epsilon^{\frac{4}{3}} \left(\frac{\eta'^2}{6K^2} + B\phi'^2 \right)}{h(0)}}. \quad (4.9)$$

The far right hand side of this equation is proportional to the total length of the string loop, from which one can see that as \mathcal{E} decreases, the constraint on the maximum length of the loop becomes tighter.

There is no explicit constraint on η (distance from the tip of the throat), since if the length of the string is zero at any point, η can be arbitrarily large. However, the length of a loop will generally be non-zero, which gives a constraint on η and confines the loop within a certain distance from the tip of the throat. From (4.9) we have:

$$\mathcal{E} \geq \mu \int d\sigma \sqrt{\frac{\mathbf{x}'^2 + h\epsilon^{\frac{4}{3}} \left(\frac{\eta'^2}{6K^2} + B\phi'^2 \right)}{h(\eta)}} \quad (4.10)$$

Again, the terms in the numerator give the length of the loop. Since h is a decreasing function of η , this equation implies that the restriction on η becomes tighter as \mathcal{E} gets smaller. Using an analytic approximation for h we can calculate the rate at which the restriction tightens. As \mathcal{E} tends towards zero (as the loop loses energy), we find that the restriction on η does not tighten as quickly as the restriction on the length of the loop. In fact, when \mathcal{E} reaches zero, the total length of the loop must be zero, whereas there is no requirement for the string to be at the bottom of the throat ($\eta = 0$). From this we argue that, in general, the length of the loop disappears before the internal motion, so it will not be localised at the tip of the throat.

Figure 8 shows the effect of the gravitational radiation damping on the simple loop Ansatz (3.8). A rather large value of damping, equivalent to setting $G\mu \simeq 10^{-7}$ in (4.8), was chosen to highlight the effect, and demonstrates nicely how the external loop radius, ρ , reduces overall more quickly than the internal oscillations. The motion towards the end of the time period becomes more and more noisy as the loop samples more the sharp valley in the effective potential at $\rho = 0$. We conclude that the emission of gravitational radiation will neither cause the string to be pulled to the tip of the throat nor the motion to become effectively 4D.

5. Discussion

In this paper, we have explored explicitly the motion of a cosmic (super)string on a compactification with warped internal dimensions, using the Klebanov-Strassler throat as a test geometry. The results show that there is no classical geometrical or dynamical mechanism which preferentially damps the motion in the internal dimensions. On the contrary, we observe a general tendency for motion in the internal

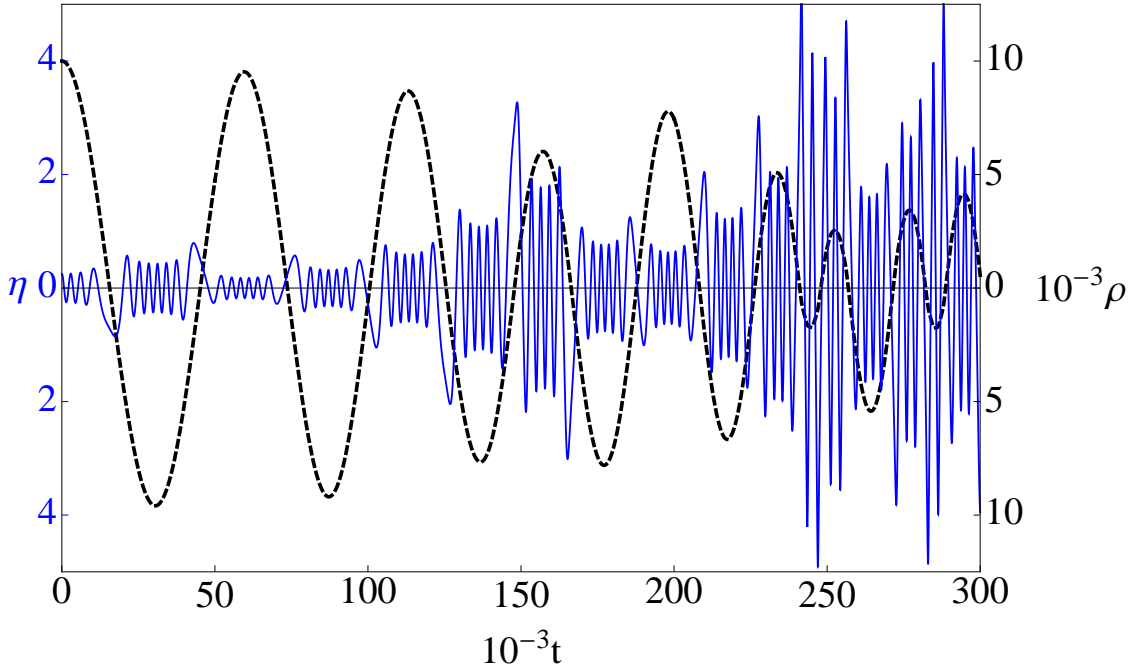


Figure 8: Including the gravitational radiation damping into the circular loops of section 3.1. The loop shown has no angular momentum, and corresponds to the damped version of the first plot in figure 1. A rather large value of damping was chosen, corresponding to a halving of E_0 by the end of the integration.

dimensions to either become or persist in being appreciable under a wide range of situations. We now discuss the ways in which motion differs from the case where the extra dimensions are flat, and how this impacts the gravitational wave signal.

Taking a flat metric allows a third gauge choice to be made along with the transverse temporal gauge, so we take the following:

$$\tau = t, \quad \dot{x}^M x'_M = 0, \quad \dot{x}^2 + x'^2 = 0.$$

The equations of motion for the string then become very simple. The trajectory in the spatial directions, which are all flat, is simply given by a wave equation:

$$\ddot{\mathbf{x}} = \mathbf{x}'' . \quad (5.1)$$

This has an analytic solution that is simply a sum of left and right-moving waves:

$$\mathbf{x}(\sigma, t) = \frac{1}{2} (\mathbf{a}(\sigma - t) + \mathbf{b}(\sigma + t)) .$$

This implies, since a closed loop must be periodic in σ , that it must also be periodic in t . The functions \mathbf{a} and \mathbf{b} can take any form subject to the following constraints

(which follow from the gauge conditions):

$$\mathbf{a}'^2 = \mathbf{b}'^2 = 1.$$

Here, prime represents differentiation by their respective arguments. Thus, with n spatial directions, these functions are constrained to lie on a unit $(n - 1)$ -sphere. This gives some interdependence between the different directions. Essentially it means that if \mathbf{a}' or \mathbf{b}' is large in one direction, it must be small in another. This is directly related to the conservation of energy, given by the condition: $\mathbf{x}'^2 + \dot{\mathbf{x}}^2 = 1$, which implies that if length or velocity terms are large in one direction, they must be small in another.

In the case of warped spacetime, loop trajectories are no longer periodic (as we see clearly on figure 1, for example). This is essentially due to the presence of two different coupled characteristic frequencies of oscillation: the characteristic frequency of the loop based on its size, and the frequency of oscillation up and down the throat, based on the scale of the throat. These two different frequencies interfere, resulting in non-periodic motion. This effect is particularly noticeable if the frequencies are comparable, which depends on the scale of the loop and the size of ϵ (which gives the scale of the throat).

In a similar way to the flat space case described above, the length and velocity terms are still constrained by the conservation of energy so that if they are large in a particular direction they must be small in another, which is expressed by the following equation:

$$\dot{\mathbf{x}}^2 + h\epsilon^{\frac{4}{3}} \left(\frac{\dot{\eta}^2}{6K^2} + B\dot{\phi}^2 \right) + \frac{\mathbf{x}'^2}{E^2 h} + \frac{\epsilon^{\frac{4}{3}}}{E^2} \left(\frac{\eta'^2}{6K^2} + B\phi'^2 \right) = 1$$

However, there is an additional interaction between the different directions that is not present in flat space. We saw in section 3.2 that motion in all directions is affected by the radial distance, η , of the string from the tip of the warped throat. We saw that if a string is close to the tip of the throat, its total length and velocity are larger, and they are smaller if the string is far from the tip. When the frequency of internal oscillations is much higher than those in the external part of the loop, which is the case for a realistic cosmological scenario, this results in more of an averaged effect (see for example figure 1), but nonetheless an important one.

The fact that some interaction between the internal radial distance and the other directions exists is apparent in the equations of motion, since the equation of motion (3.4) for the internal radial distance, η , contains terms depending on all the other directions, while the other equations of motion, (3.5) and (3.3), depend on η . In (5.1), we see that no such dependence appears in flat spacetime.

This all means that strings in warped spacetime have more interesting and complex motion than those in flat spacetime, and we have seen a few examples of their

intriguing dynamics in this paper (see for example figures 3 and 4). The main conclusion is that the warped geometry will also contain appreciable internal motion which will then impact on the physics of the 4D cosmological network.

In [39, 40], it was shown that if there was a portion of kinetic energy in the internal dimensions, then the string would slow down in our external noncompact dimensions. This then feeds into a reduced gravitational wave signal as the energy-momentum of the string,

$$T^{\mu\nu} = \mu \int d^2\sigma (\dot{X}^\mu \dot{X}^\nu - X'^\mu X'^\nu) \delta^{(4)}(x^\mu - X^\mu(\tau, \sigma)), \quad (5.2)$$

is sharply peaked in fourier space around the wave vectors of the left and right moving modes. It is only when these wave vectors either coincide (as in a cusp) or one has a discontinuity (as in a kink) that the contribution to the linearized gravitational wave is enhanced. If the wave vectors cease to be null, then there is a corresponding lowering of the overall power in a gravitational wave burst, as well as a narrowing of the region in which it is beamed. The near cusp event parameter, Δ , measuring how close to relativistic the wave velocities of the string are, is the parameter which governs the reduction in the signal.

In this paper we explored the values of Δ for a family of simple loops, where we could identify where the string was moving at its most relativistically. This gave sample data for Δ which ranged (roughly) from $10^{-2} - 10^{-3}$. In [40], the overall effect on the gravitational wave signal for cusps was obtained by marginalising over the Δ parameter up to a maximum value Δ_0 . The results here indicate that $\Delta_0 \sim 10^{-3}$ might be a conservative but sensible value to take, in which case (referring to figure 6 of [40]), we see that the expected detection rate of a cusp event is likely to be around 1 per century!

Acknowledgments

We would like to thank Louis Leblond for helpful discussions. AA is supported by a Marie Curie IEF Fellowship at the the University of Nottingham. SC is supported by an EPSRC studentship. RG is supported in part by STFC (Consolidated Grant ST/J000426/1), in part by the Wolfson Foundation and Royal Society, and in part by Perimeter Institute for Theoretical Physics. Research at Perimeter Institute is supported by the Government of Canada through Industry Canada and by the Province of Ontario through the Ministry of Economic Development and Innovation. AA and SC would like to acknowledge the support of the CTC at Cambridge, and also SC the hospitality of the Perimeter Institute during the course of this project.

References

- [1] A. Vilenkin, Phys. Rept. **121**, 263 (1985).

- M. B. Hindmarsh and T. W. B. Kibble, Rept. Prog. Phys. **58**, 477 (1995) [arXiv:hep-ph/9411342].
- [2] Y. B. Zeldovich, I. Y. Kobzarev and L. B. Okun, Zh. Eksp. Teor. Fiz. **67**, 3 (1974) [Sov. Phys. JETP **40**, 1 (1974)].
T. W. B. Kibble, J. Phys. A **9**, 1387 (1976).
- [3] A. J. Albrecht, R. A. Battye and J. Robinson, Phys. Rev. Lett. **79**, 4736 (1997) [arXiv:astro-ph/9707129].
- [4] C. Contaldi, M. Hindmarsh and J. Magueijo, Phys. Rev. Lett. **82**, 2034 (1999) [astro-ph/9809053].
- [5] G. R. Dvali and S. H. H. Tye, Phys. Lett. B **450**, 72 (1999) [arXiv:hep-ph/9812483].
S. H. S. Alexander, Phys. Rev. D **65**, 023507 (2002) [arXiv:hep-th/0105032].
C. P. Burgess, M. Majumdar, D. Nolte, F. Quevedo, G. Rajesh and R. J. Zhang, JHEP **0107**, 047 (2001) [arXiv:hep-th/0105204].
G. Shiu and S. H. H. Tye, Phys. Lett. B **516**, 421 (2001) [arXiv:hep-th/0106274];
- [6] S. Kachru, R. Kallosh, A. D. Linde, J. M. Maldacena, L. P. McAllister and S. P. Trivedi, JCAP **0310**, 013 (2003) [arXiv:hep-th/0308055].
- [7] S. H. Henry Tye, Lect. Notes Phys. **737**, 949 (2008) [arXiv:hep-th/0610221].
J. M. Cline, “String cosmology,” arXiv:hep-th/0612129.
R. Kallosh, Lect. Notes Phys. **738**, 119 (2008) [arXiv:hep-th/0702059].
C. P. Burgess, Class. Quant. Grav. **24**, S795 (2007) [arXiv:0708.2865 [hep-th]].
L. McAllister and E. Silverstein, Gen. Rel. Grav. **40**, 565 (2008) [arXiv:0710.2951 [hep-th]].
- [8] S. Sarangi and S. H. H. Tye, Phys. Lett. B **536**, 185 (2002) [arXiv:hep-th/0204074].
G. Dvali and A. Vilenkin, Phys. Rev. D **67**, 046002 (2003) [arXiv:hep-th/0209217].
G. Dvali and A. Vilenkin, JCAP **0403**, 010 (2004) [arXiv:hep-th/0312007].
- [9] N. T. Jones, H. Stoica and S. H. H. Tye, Phys. Lett. B **563** (2003) 6 [arXiv:hep-th/0303269].
E. J. Copeland, R. C. Myers and J. Polchinski, JHEP **0406**, 013 (2004) [arXiv:hep-th/0312067].
- [10] E. J. Copeland, L. Pogosian and T. Vachaspati, Class. Quant. Grav. **28**, 204009 (2011) [arXiv:1105.0207 [hep-th]].
- [11] M. Hindmarsh, Prog. Theor. Phys. Suppl. **190** (2011) 197 [arXiv:1106.0391 [astro-ph.CO]].
- [12] E.P.S.Shellard, Nucl. Phys. B **283**, 624 (1987). K.Moriarty, E.Myers and C.Rebbi, Phys. Lett. B **207**, 411 (1988).
- [13] D. Forster, Nucl. Phys. B **81**, 84 (1974).

- [14] R. Gregory, Phys. Lett. B **206**, 199 (1988).
R. Gregory, D. Haws and D. Garfinkle, Phys. Rev. D **42**, 343 (1990).
- [15] T. Vachaspati, A. E. Everett and A. Vilenkin, Phys. Rev. D **30**, 2046 (1984).
C. J. Burden, Phys. Lett. B **164**, 277 (1985).
T. Vachaspati, Phys. Rev. D **35** (1987) 1767.
- [16] T. Vachaspati and A. Vilenkin, Phys. Rev. D **31**, 3052 (1985).
- [17] B. Allen and E. P. S. Shellard, Phys. Rev. Lett. **64**, 119 (1990).
D. P. Bennett and F. R. Bouchet, Phys. Rev. D **41**, 2408 (1990).
- [18] J. Polchinski, “Introduction to cosmic F- and D-strings,” arXiv:hep-th/0412244.
E. J. Copeland and T. W. B. Kibble, “Cosmic Strings and Superstrings,” arXiv:0911.1345 [Unknown].
- [19] J. Polchinski, Phys. Lett. B **209**, 252 (1988).
M. G. Jackson, N. T. Jones and J. Polchinski, JHEP **0510**, 013 (2005) [arXiv:hep-th/0405229].
A. Hanany and K. Hashimoto, JHEP **0506**, 021 (2005) [arXiv:hep-th/0501031].
- [20] M. Sakellariadou, JCAP **0504** (2005) 003 [hep-th/0410234].
- [21] A. Avgoustidis and E. P. S. Shellard, Phys. Rev. D **73**, 041301 (2006) [arXiv:astro-ph/0512582].
- [22] E. J. Copeland, T. W. B. Kibble and D. A. Steer, Phys. Rev. D **75** (2007) 065024 [arXiv:hep-th/0611243].
E. J. Copeland, T. W. B. Kibble and D. A. Steer, Phys. Rev. Lett. **97** (2006) 021602 [arXiv:hep-th/0601153].
E. J. Copeland, H. Firouzjahi, T. W. B. Kibble and D. A. Steer, Phys. Rev. D **77** (2008) 063521 [arXiv:0712.0808 [hep-th]].
N. Bevis and P. M. Saffin, Phys. Rev. D **78** (2008) 023503 [arXiv:0804.0200 [hep-th]].
- [23] A. C. Davis, W. Nelson, S. Rajamanoharan and M. Sakellariadou, JCAP **0811**, 022 (2008) [arXiv:0809.2263 [hep-th]].
R. Brandenberger, H. Firouzjahi, J. Karouby and S. Khosravi, JCAP **0901**, 008 (2009) [arXiv:0810.4521 [hep-th]].
P. Binetruy, A. Bohe, T. Hertog and D. A. Steer, Phys. Rev. D **80**, 123510 (2009) [arXiv:0907.4522 [hep-th]].
- [24] N. Bevis, E. J. Copeland, P. Y. Martin, G. Niz, A. Pourtsidou, P. M. Saffin and D. A. Steer, Phys. Rev. D **80**, 125030 (2009) [arXiv:0904.2127 [hep-th]].
H. Firouzjahi, J. Karouby, S. Khosravi and R. Brandenberger, Phys. Rev. D **80**, 083508 (2009) [arXiv:0907.4986 [hep-th]].
- [25] S. H. Tye, I. Wasserman and M. Wyman, Phys. Rev. D **71** (2005) 103508 [Erratum-ibid. D **71** (2005) 129906] [arXiv:astro-ph/0503506].

- A. Avgoustidis and E. P. S. Shellard, Phys. Rev. D **78** (2008) 103510 [arXiv:0705.3395 [astro-ph]].
- A. Avgoustidis and E. J. Copeland, Phys. Rev. D **81** (2010) 063517 [arXiv:0912.4004 [hep-ph]].
- [26] M. Hindmarsh and P. M. Saffin, JHEP **0608** (2006) 066 [arXiv:hep-th/0605014].
A. Rajantie, M. Sakellariadou and H. Stoica, JCAP **0711**, 021 (2007) [arXiv:0706.3662 [hep-th]].
J. Urrestilla and A. Vilenkin, JHEP **0802**, 037 (2008) [arXiv:0712.1146 [hep-th]].
- [27] A. Pourtsidou, A. Avgoustidis, E. J. Copeland, L. Pogosian and D. A. Steer, Phys. Rev. D **83**, 063525 (2011) [arXiv:1012.5014 [astro-ph.CO]].
A. Avgoustidis, E. J. Copeland, A. Moss, L. Pogosian, A. Pourtsidou and D. A. Steer, Phys. Rev. Lett. **107** (2011) 121301 [arXiv:1105.6198 [astro-ph.CO]].
- [28] T. W. B. Kibble and N. Turok, Phys. Lett. B **116**, 141 (1982).
N. Turok, Nucl. Phys. B **242**, 520 (1984).
- [29] A. Avgoustidis and E. P. S. Shellard, Phys. Rev. D **71**, 123513 (2005) [arXiv:hep-ph/0410349].
- [30] N. K. Nielsen, Nucl. Phys. B **167** (1980) 249.
- [31] E. Witten, Nucl. Phys. B **249** (1985) 557.
- [32] A. Vilenkin and E.P.S. Shellard, *Cosmic Strings and Other Topological Defects* (Cambridge University Press, 1994)
- [33] B. Allen and R. R. Caldwell, Phys. Rev. Lett. **65** (1990) 1705.
B. Allen and R. R. Caldwell, Phys. Rev. D **43** (1991) 3173.
- [34] D. Garfinkle and T. Vachaspati, Phys. Rev. D **36**, 2229 (1987).
- [35] F. S. Accetta and L. M. Krauss, Nucl. Phys. B **319**, 747 (1989).
R. J. Scherrer, J. M. Quashnock, D. N. Spergel and W. H. Press, Phys. Rev. D **42**, 1908 (1990).
M. Sakellariadou, Phys. Rev. D **42**, 354 (1990) [Erratum-ibid. D **43**, 4150 (1991)].
- [36] J. M. Quashnock and D. N. Spergel, Phys. Rev. D **42**, 2505 (1990).
B. Allen and E. P. S. Shellard, Phys. Rev. D **45**, 1898 (1992).
B. Allen, P. Casper and A. Ottewill, Phys. Rev. D **50**, 3703 (1994) [arXiv:gr-qc/9405037].
- [37] T. Damour and A. Vilenkin, Phys. Rev. D **64** (2001) 064008 [arXiv:gr-qc/0104026].
T. Damour and A. Vilenkin, Phys. Rev. D **71** (2005) 063510 [arXiv:hep-th/0410222].
- [38] F. A. Jenet *et al.*, Astrophys. J. **653**, 1571 (2006) [arXiv:astro-ph/0609013].
B. P. Abbott *et al.* [LIGO Scientific Collaboration], Phys. Rev. D **80**, 062002 (2009) [arXiv:0904.4718 [astro-ph.CO]].

- [39] E. O’Callaghan, S. Chadburn, G. Geshnizjani, R. Gregory and I. Zavala, Phys. Rev. Lett. **105**, 081602 (2010) [arXiv:1003.4395 [hep-th]].
E. O’Callaghan and R. Gregory, JCAP **1103**, 004 (2011) [arXiv:1010.3942 [hep-th]].
- [40] E. O’Callaghan, S. Chadburn, G. Geshnizjani, R. Gregory and I. Zavala, JCAP **1009**, 013 (2010) [arXiv:1005.3220 [hep-th]].
- [41] A. Avgoustidis, Phys. Rev. D **78**, 023501 (2008) [arXiv:0712.3224 [hep-th]].
- [42] I. R. Klebanov and M. J. Strassler, JHEP **0008**, 052 (2000) [arXiv:hep-th/0007191].
- [43] P. Candelas and X. C. de la Ossa, Nucl. Phys. B **342**, 246 (1990).
R. Minasian and D. Tsimpis, Nucl. Phys. B **572**, 499 (2000) [arXiv:hep-th/9911042].
C. P. Herzog, I. R. Klebanov and P. Ouyang, “Remarks on the warped deformed conifold,” arXiv:hep-th/0108101.
- [44] D. Baumann and L. McAllister, Phys. Rev. D **75**, 123508 (2007) [hep-th/0610285].
- [45] R. Gregory and D. Kaviani, JHEP **1201**, 037 (2012) [arXiv:1107.5522 [hep-th]].
- [46] J. J. Blanco-Pillado and A. Iglesias, JHEP **0508**, 040 (2005) [hep-th/0504068].
- [47] M. Lake, S. Thomas and J. Ward, JCAP **1001**, 026 (2010) [arXiv:0911.3118 [hep-ph]].
- [48] C. J. A. P. Martins and E. P. S. Shellard, Phys. Rev. D **54**, 2535 (1996) [arXiv:hep-ph/9602271 [hep-ph]].
- [49] T. W. B. Kibble, Nucl. Phys. B **252**, 227 (1985) [Erratum-ibid. B **261**, 750 (1985)].
- [50] U. F. Wichoski, J. H. MacGibbon and R. H. Brandenberger, Phys. Rev. D **65**, 063005 (2002) [hep-ph/9805419].
P. Bhattacharjee and N. C. Rana, Phys. Lett. B **246**, 365 (1990).
- [51] J. J. Blanco-Pillado, K. D. Olum and B. Shlaer, Phys. Rev. D **83**, 083514 (2011) [arXiv:1101.5173 [astro-ph.CO]].
- [52] C. J. A. P. Martins and E. P. S. Shellard, Phys. Rev. D **73** (2006) 043515 [astro-ph/0511792].
- [53] C. Ringeval, M. Sakellariadou and F. Bouchet, JCAP **0702** (2007) 023 [astro-ph/0511646].
L. Lorenz, C. Ringeval and M. Sakellariadou, JCAP **1010** (2010) 003 [arXiv:1006.0931 [astro-ph.CO]].
- [54] K. D. Olum and V. Vanchurin, Phys. Rev. D **75** (2007) 063521 [astro-ph/0610419].
V. Vanchurin, K. D. Olum and A. Vilenkin, Phys. Rev. D **74** (2006) 063527 [gr-qc/0511159].

- [55] D. A. Steer and T. Vachaspati, Phys. Rev. D **83**, 043528 (2011) [arXiv:1012.1998 [hep-th]].
- [56] H. Firouzjahi, Phys. Rev. D **77**, 023532 (2008) [arXiv:0710.4609 [hep-th]].
- [57] J. -F. Dufaux, arXiv:1109.5121 [hep-th].
J. -F. Dufaux, arXiv:1201.4850 [hep-th].
- [58] R. J. Scherrer, J. M. Quashnock, D. N. Spergel and W. H. Press, Phys. Rev. D **42**, 1908 (1990).